

CHAPTER 3

METHODOLOGY

Since this research mainly focuses on characteristic of dynamic model of IIR-SOFC during transient process, it is necessary to investigate both kinetic and thermodynamic behavior of the system. The steam reforming rate expressions and thermodynamic model of the IIR-SOFC system are integrated in order to predict the temperature profile of the reformer and the SOFC stack. This mathematical model is established by using COMSOL.

3.1 Mathematical model of the IIR-SOFC study

3.1.1 Model geometry

To investigate a model to predict the temperature distribution with each operating time of the IIR-SOFC system, firstly, it is necessary to establish the geometry (monolithic, planar, or tubular). In this study, the system was fabricated in tubular design. It is noted that the effect of momentum, mass, heat and ionic transport by the time in the system had to integrate together.

Schematic diagram of tubular-designed IIR-SOFC with coated-wall reformer are shown in Fig 3.1. According to this configuration, primary fuels are converted to hydrogen-rich gas at internal reformer before introduced to fuel channel of tubular SOFC. Simultaneously, air is fed with opposite flow direction through air channel. It is noted that all dimensions and physical properties of SOFC system in the present work, which are summarized in Table 3.1, are based on previous reports from literatures [Costamagna *et al*, 2004; Xue *et al*, 2005; Zhu *et al*, 2006].

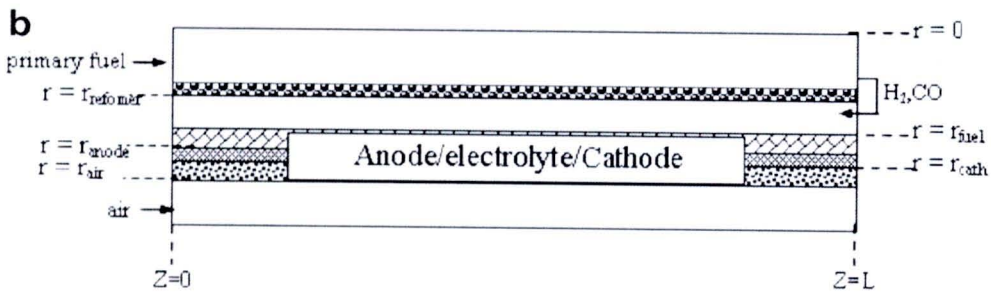


Figure 3.1 Schematic view of IIR-SOFC with indirect internal reforming with coated-wall reformer

Table 3.1 Dimension and constant parameter values of tubular IIR-SOFC system

Parameter	Value	Reference
Fuel cell length	0.60 m	Zhu <i>et al</i> , 2006
Reformer radius	2×10^{-3} m	Zhu <i>et al</i> , 2006
Inside radius of the cell	5.4×10^{-3} m	Zhu <i>et al</i> , 2006
Anode thickness	1×10^{-3} m	Zhu <i>et al</i> , 2006
Electrolyte thickness	4×10^{-5} m	Zhu <i>et al</i> , 2006
Cathode thickness	5×10^{-5} m	Zhu <i>et al</i> , 2006
Anode permeability	1×10^{-12} m	Costamagna <i>et al</i> , 2004
Cathode permeability	1×10^{-12} m	Costamagna <i>et al</i> , 2004
Average density of triple phase	633.73 kg/m ³	Xue <i>et al</i> , 2005
Average specific heat of triple phase	574.3 J/kg/K	Xue <i>et al</i> , 2005
Convection coefficient in the fuel channel	2,987 W/m ² /K	Xue <i>et al</i> , 2005
Convection coefficient in the air channel	1,322.8 W/m ² /K	Xue <i>et al</i> , 2005

3.1.2 Model assumption and equations

The model was developed as the smallest unit cell taking into account the effect of temperature on gas distribution, reactant conversion. All assumptions made are:

- Each section is considered as non-isothermal transient conditions.
- Ideal gas behavior is applied for all gas components.
- Pressure drop in SOFC stack and coated-wall reformer are neglected.
- Fuel utilization was fixed constantly at 80% along the cell coordinate.
- Radiation is neglected.

A number of equations were applied to predict concentration and temperature gradients along this tubular IIR-SOFC system. Details for these set of equations were present in chapter 2. The boundary conditions of the state 2-D dimensional tubular SOFC model were presented in Table 3.2

Table 3.2 Transient 2-D dimensional model for tubular coated-wall reformer

Coated-wall reforming model		
Mass balance	$\frac{\delta c_i}{\delta t} + \nabla \cdot (-D_i \nabla c_i) = R_i - u \nabla \cdot c_i$	(3.1)
Energy Balance	$\rho C_p \left(\frac{\delta T}{\delta t} + u \cdot \nabla T \right) = \nabla \cdot (k \nabla T) + Q$	(3.2)
Momentum Balance	$\rho \frac{\delta u}{\delta t} + \rho(u \cdot \nabla)u = \nabla[-pI + \eta(\nabla u + (\nabla u)^T)]$	(3.3)
Fuel Channel and Air Channel		
Mass Balance	$\frac{\delta c_i}{\delta t} + \nabla \cdot (-D_i \nabla c_i) = 0$	(3.5)
Energy Balance	$\rho C_p \left(\frac{\delta T}{\delta t} + u \cdot \nabla T \right) = \nabla \cdot (k \nabla T) + Q$	(3.6)
Momentum Balance	$\rho \frac{\delta u}{\delta t} + \rho(u \cdot \nabla)u = \nabla[-pI + \eta(\nabla u + (\nabla u)^T)]$	(3.7)
Solid cell		
Energy Balance	$\rho C_p \left(\frac{\delta T}{\delta t} \right) - \nabla \cdot (k \nabla T) = Q$	(3.8)

3.1.3 Model description

Model consists of reformer section, fuel channel, solid state and air channel. Solid state consists of anode, electrolyte and cathode that shown in figure 3.2. Boundary condition of this model separated by sub domain are shown in table 3.4 and initial conditions are shown in table 3.3

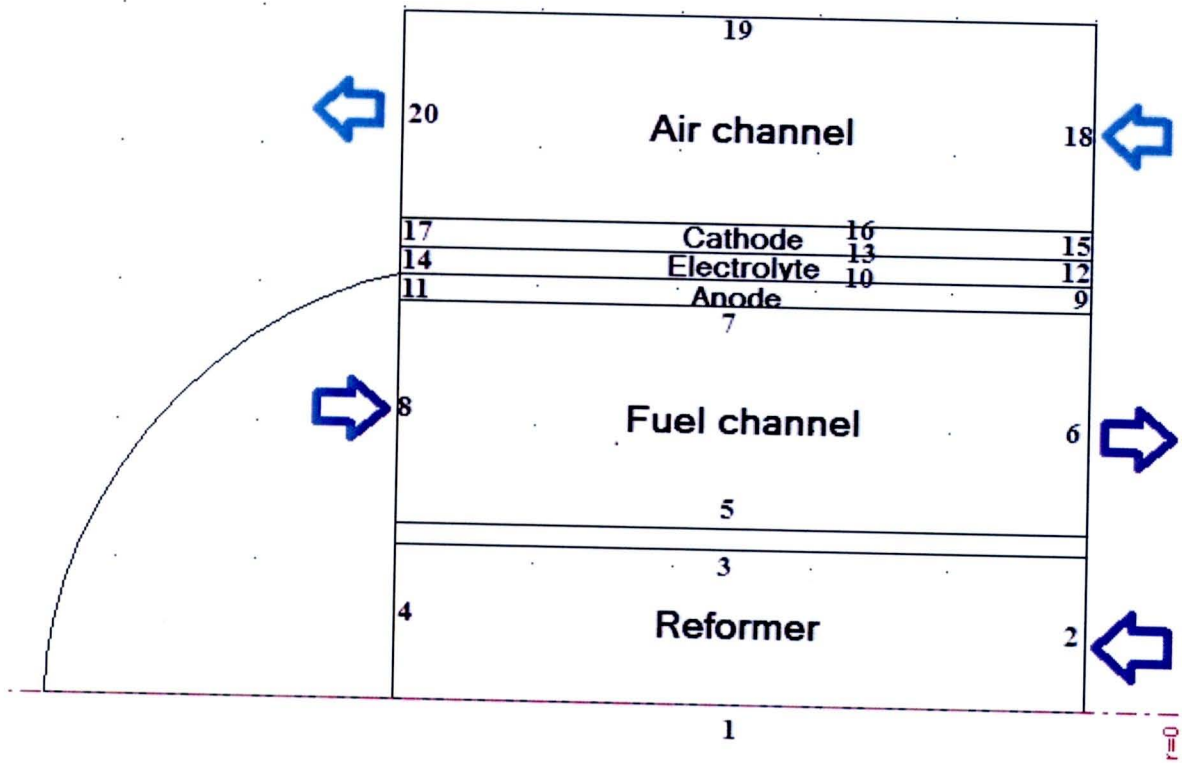


Figure 3.2 Schematic model of IIR-SOFC with boundary number

Table 3.3 Initial condition

Parameters	Variable
Pressure	1 bar
Initial cell temperature	500 K
Inlet gases temperature	1173 K
Inlet gas velocity	3.04e-3 m/s

Table 3.4 Boundary condition for tubular IIR-SOFC

Boundary	Momentum Balance	Mass Balance	Energy Balance
Reformer section			
1	Axial Symmetry	Axial Symmetry	Axial Symmetry
2	Inlet velocity	Inlet concentration	Inlet Temperature
3	Wall	Flux	Heat Flux
4	Outlet	Outlet	Outlet
Fuel channel			
5	Wall	Wall	Conduction
6	Outlet	Outlet	Outlet
7	Open boundary	Continuity	Continuity
8	Inlet	Inlet	Inlet
Anode			
9	Outlet	Outlet	Outlet
10	Wall	Flux	Heat generation
11	Inlet	Inlet	Inlet
Electrolyte			
12	Wall	Wall	Thermal insulation



13	Wall	Flux	Conduction
14	Wall	Wall	Thermal insulation
Cathode			
15	Inlet	Inlet	Inlet
16	Open boundary	Inlet	Convection
17	Outlet	Outlet	Outlet
Air channel			
18	Inlet	Inlet	Inlet
19	Wall	Wall	Thermal Insulation
20	Outlet	Outlet	Outlet

3.2 Framework Study

According to the aim of this study, mathematical models were developed under several operating patterns. Several sets of equations were investigated in order to simulate the case studied.

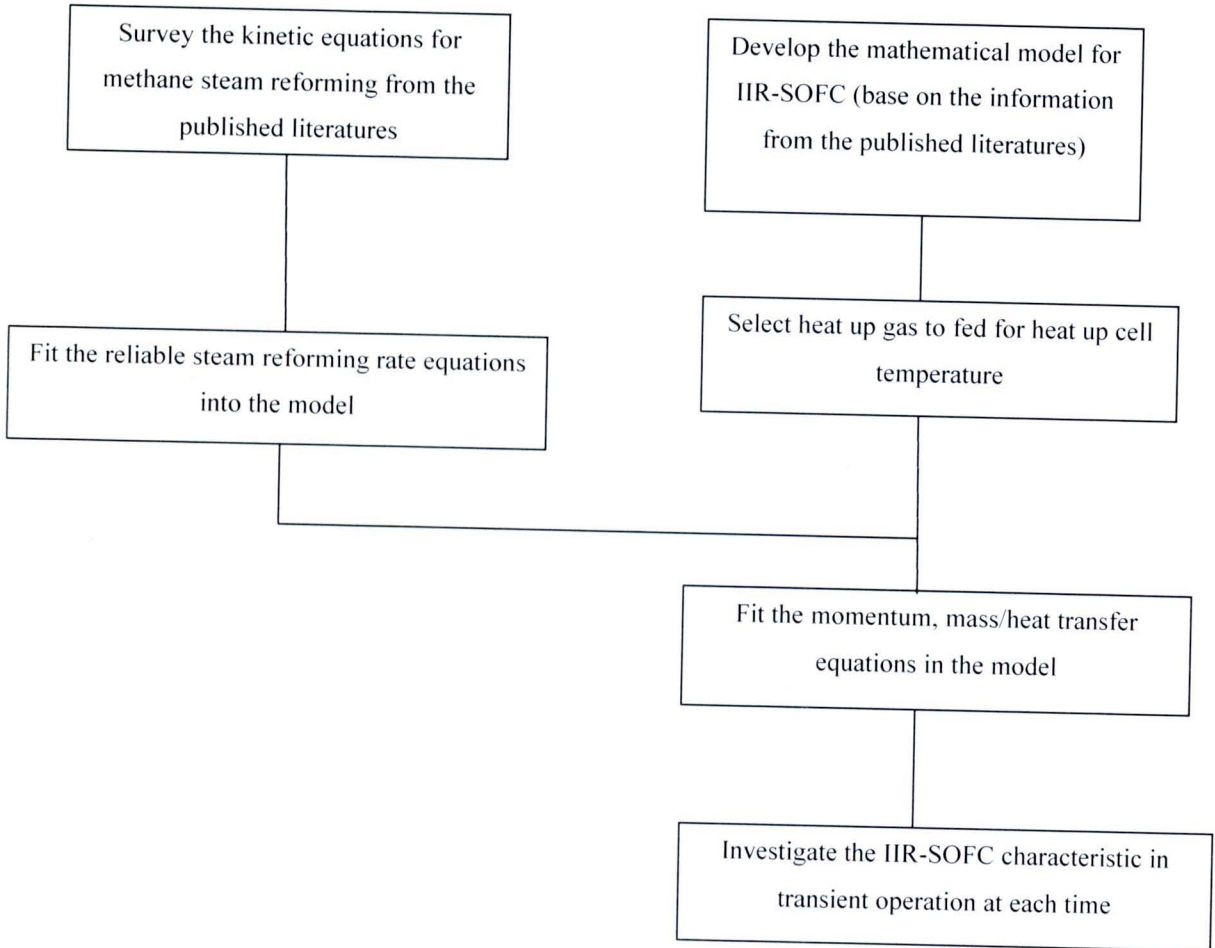


Figure 3.2 Framework of this study

3.3 Governing Equation

According to its structure, each IIR-SOFC component can be separated into porous media and non-porous media. For porous structures, its porosity, tortuosity and permeability properties of the material that normally affect the transport behaviors of gases. Finally, all developed models in this study are calculated based on the algorithm in Fig 3.3

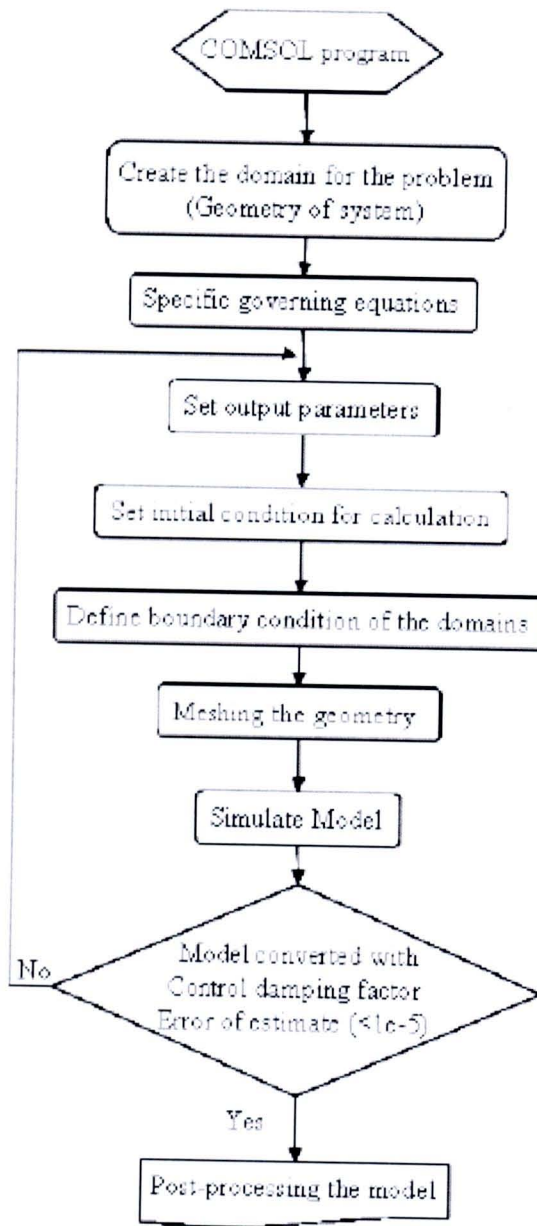


Figure 3.3 Flow diagram of coded procedure for COMSOL®